Tritschler, U., Gwyther, J., Harniman, R., Whittell, G. R., Winnik, M. A., & Manners, I. (2018). Toward Uniform Nanofibers with a -Conjugated Core: Optimizing the "Living" Crystallization-Driven Self-Assembly of Diblock Copolymers with a Poly(3-octylthiophene) Core-Forming Block. *Macromolecules*, *51*(14), 5101-5113. https://doi.org/10.1021/acs.macromol.8b00488

Towards Uniform Nanofibers with a π-Conjugated Core: Optimising the "Living" Crystallization-Driven Self-Assembly of Diblock Copolymers with a Poly(3-octylthiophene) Core-Forming Block

Ulrich Tritschler,[†] Jessica Gwyther,[†] Robert L. Harniman,[†] George R. Whittell,[†] Mitchell A. Winnik,[‡] and Ian Manners[†,*]

[†]School of Chemistry, University of Bristol, Bristol, BS8 1TS (UK)

[‡]Department of Chemistry, University of Toronto, Toronto M5S 1A1, Ontario, Canada.

Corresponding Author

*E-mail: ian.manners@bristol.ac.uk (I.M.).

Abstract.

Crystalline poly(3-alkylthiophene) (P3AT) nanofibers are promising materials for a myriad of device applications but nanofiber length control and colloidal stability are difficult to achieve. We report an in depth study of the solution self-assembly of regioregular poly(3-octylthiophene)-*b*-poly(dimethylsiloxane) (P3OT-*b*-PDMS) diblock copolymers with a crystallizable p-conjugated core-forming block. Use of "living" crystallization-driven self-assembly (CDSA) seeded-growth method in solvents selective for PDMS allowed access to relatively low length dispersity, colloidally stable P3OT-*b*-PDMS fiber-like micelles with a crystalline, tape-like P3OT core and a PDMS corona and lengths up to ca. 600 nm under optimised conditions. Significantly, the presence of a small percentage of common solvent and the use of slightly elevated temperature (35°C) was found to enhance the length control. Analogous studies for P3OT-*b*-PS (PS = polystyrene) suggest that solvent composition and temperature represent key parameters for the general optimisation of fiber formation by living CDSA for P3AT block copolymers.

Introduction

One-dimensional (1D) nanofibers composed of π-conjugated, semiconducting homopolymers are currently of major interest as active components of devices, for example as solution-processable components for organic photovoltaics due to their high carrier mobility. In particular, regioregular poly(3-alkylthiophene)s (P3ATs), such as poly(3-hexylthiophene) (P3HT), are promising as they possess desirable optoelectronic properties.[1-7] An essential parameter for high performance photovoltaic devices is a high hole mobility, which is provided by crystalline P3AT nanofibers.[3, 4, 8] Further applications as emissive and conductive nanowires with a, crystalline, π-conjugated nanofiber core have also been reported.[6, 9] However, the lack of colloidal stability complicates solution processing and the near absence of fiber length control hinders device optimisation.

The solution self-assembly of block copolymers (BCPs) in block selective solvents is a versatile route to core-shell micellar nanoparticles with different morphologies, such as spheres, cylinders or fibers, and vesicles.[10-22] Until recently, the vast majority of studies focused on the use of core-forming blocks that were amorphous and in such cases fiber-like structures comprise only a very restricted region of the phase space, and are often mixed with other morphologies. In addition, no access to samples with controlled lengths and low length polydispersities was possible. Recent work has shown that the presence of a crystalline core generally promotes the formation of micelles with low interfacial curvature such as 1D fibers or 2D platelets. For example, BCPs with a crystallizable poly(ferrocenyldimethylsilane)[23] core-forming block form fiber-like micelles for a range of block ratios from 1:3 to 1:20.[23, 24] The formation of fiber-like micelles with crystalline cores has also been achieved for other BCPs with crystallisable core-forming blocks, such as PE,[25-28] PEO,[29] polycaprolactone,[30-32] poly(L-lactic acid),[33-38] poly(3-hexylthiophene),[39-45] poly(3-heptylselenophene),[46] oligo- and poly(phenylene-vinylene),[47-49] and poly(dialkylfluorene).[50-52] Moreover, in an expanding number of cases the formation of low dispersity 1D fibers with length control can be achieved by a method termed "living" crystallization-driven self-assembly (CDSA). This seeded growth method relies on the formation of small seed micelles by sonication of long polydisperse fibers.[53] Addition of BCP unimer (molecularly dissolved block copolymer) then leads to epitaxial growth from the seed termini. The increase in micelle length can result in structures with lengths of over 2 microns and is dependent on the

seed-to-unimer ratio. Furthermore, the samples are monodisperse in length and the process in many regards is analogous to a living covalent polymerization of molecular monomers.[53-56] An alternative approach to the generation of seed micelles is termed "self-seeding" and involves the partial dissolution of fiber-like micelles due to the presence of crystallites of different sizes in the core. This can either be achieved thermally or by the use of media containing significant amounts (e.g. between 10 and 17 % by volume) of a common solvent for both blocks. On cooling, or on evaporation of the common solvent, the released unimer will then add to the remaining seeds.[57, 58] Micelle length control is possible using the self-seeding approach, but thermal processing requires the generation of a calibration curve that is dependent on the micelle sample history as this can influence the crystallinity of the core. Living CDSA has permitted the fabrication of monodisperse fibers that form lyotropic liquid crystalline phases,[59, 60] and via the sequential addition of different BCP unimers, segmented 1D block comicelles,[54, 61] including amphiphilic examples[62] and spatially distinct regions of hydrogen-bonding donors and acceptors that hierarchically self-assemble into supermicelles.[63, 64] Moreover, the living CDSA, seeded growth approach has been extended beyond crystallizable BCPs[25, 34, 48, 49, 65, 66] to crystallisable homopolymers with charged termini[67, 68] and to molecular species[69-76] that form stacked structures by π- or hydrogen bonding interactions, and also to 2 dimensions to yield platelet micelles with controlled dimensions and complexity.[32, 77-79]

The solution self-assembly of P3AT-containing diblock copolymers (diBCPs) has attracted considerable attention as a method by which to prepare colloidally stable functional nanoparticles. The formation of various micellar morphologies, such as spheres,[44, 80, 81] fibers,[41, 43, 44] vesicles,[81] and helical structures[45] has been reported, in addition to hierarchical structures such as bundles and branched superstructures,[43] stars and networks,[82] and coaxial hybrid nanowires containing quantum dots.[83] In order to transpose the fiber length and architectural control characteristic of the living CDSA method to P3AT BCPs we have explored the seeded growth of fiber-like micelles with a crystalline, π-conjugated P3HT core. Although addition of P3HT-*b*-PDMS (block ratio 1:11, PDMS = poly(dimethylsiloxane)) to small (L_n = 38 nm) seed micelles created by the sonication of preformed polydisperse fibers formed from the same BCP led to growth, this was limited to a maximum length of only ca. 250 nm, and was characterised by very inefficient uptake at the seed termini.[41] Studies of P3HT-*b*-PMMA (PMMA =

poly(methylmethacrylate)) highlighted the issue of facile spontaneous (homogeneous) nucleation for P3HT BCPs, which generates new micelles, and can compete with seeded growth.[40] Improved results were obtained for the seeded growth of P3HT-*b*-P2VP (P2VP = poly(2-vinylpyridine)) with much higher unimer uptake and access to fibers of length up to ca. 300 nm and with low length polydispersities of < 1.11. However, attempts to form longer fibers were unsuccessful, and it appears that the rapid crystallization of P3HT can introduce defects in the micelle core that reduce and ultimately prevent epitaxial growth from the termini. This was supported by the successful formation of P3HT-*b*-PS fibers with length up to 700 nm by thermal self-seeding at 55 – 65°C, where the ability for the core to reorganize and lower the number of defects by annealing was proposed.[42] Moreover, the resulting fibers were active to further growth allowing access to block comicelles via the addition of P3HT-*b*-PDMS.[42] Thermal self-seeding has also recently been used to access uniform P3HT BCP nanofibers with lengths up to ca. 1 μm with applications in field effect transistors.[84, 85]

In this study, we return to the seeded growth approach because of the ease of implementation and report detailed studies of BCPs with a different crystallisable P3AT core-forming block, poly(3-octylthiophene) (P3OT). The increased side chain length was adopted in an attempt to increase solubility and to slow down the face-to-face packing during the solution self-assembly, which is driven through intermolecular π-π interactions.[86-88] Such a reduction in the crystallization rate might be anticipated to reduce the formation of defects in the crystalline core thereby increasing the efficiency of seeded growth. Specifically, we describe the synthesis, characterization, solution self-assembly, and seeded growth of P3OT-*b*-PDMS diBCPs with different block ratios (1:0.5, 1:2, and 1:5). We have optimized this system using key principles emerging from previous self-assembly studies for P3HT BCPs, such as the advantage of the presence of common solvent to suppress competition from homogenous nucleation during seeded growth.[39, 40] Furthermore, we have identified the important role of a slightly elevated temperature in facilitating living CDSA for these materials.[89] Finally, we have applied our findings to P3OT-*b*-PS diBCPs, revealing that the presence of common solvent and slightly elevated temperature provides a general strategy for improved seeded growth of P3AT BCPs.

Results and Discussion

1. Synthesis and structural characterization of P3OT-*b*-PDMS diblock copolymers. A series of P3OT-*b*-PDMS diBCPs with different block length ratios, but with the P3OT block length constant were synthesized (block ratios of ca. P3OT:PDMS = 1:0.5, 1:2, and 1:5). These materials were prepared by Cu-catalyzed azide-alkyne cycloaddition reactions of alkyne-terminated P3OT and azide-terminated PDMS homopolymers, both synthesized in previous steps (see Scheme 1, for characterization data, see the supporting information).

Scheme 1. Synthesis of P3OT-*b*-PDMS.

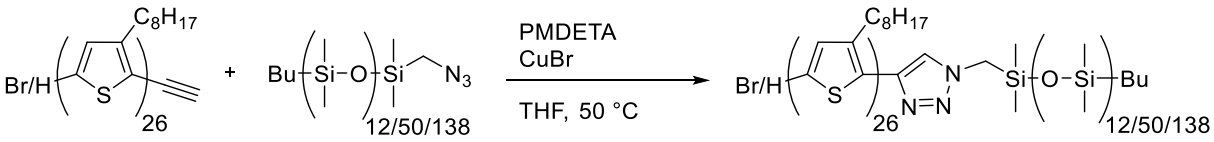

The regioregular alkyne-terminated P3OT block was synthesized via the Grignard metathesis route according to previous methods,[90-92] using ethynylmagnesium bromide to quench the chain growth polymerization. The molecular structure of the alkyne-end functionalized P3OT homopolymer was characterized by ^{1}H NMR spectroscopy (see Figure S1 in the Supporting Information (SI)). The number-average molar mass M_n of the P3OT homopolymers was found to be 5200 g mol^{-1} by matrix-assisted laser desorption/ionisation - time of flight (MALDI-TOF) mass spectroscopy, corresponding to a number-average degree of polymerization, DP_n, of 26. The polydispersity (PDI = M_w/M_n) of the P3OT homopolymer was determined by gel permeation chromatography (GPC) (PDI = 1.07). The percentage of mono-capped alkyne end-functionalization was 76%, as determined by MALDI-TOF mass spectroscopy.

The azide-terminated PDMS blocks were synthesized in two steps as reported previously.[93] The anionic polymerization of hexamethylcyclotrisiloxane was initiated with *n*-butyl lithium and terminated with (bromomethyl)chlorodimethylsilane, followed by azide functionalisation of the bromo-terminated PDMS chain ends with sodium azide. The PDMS homopolymers were characterized by ^{1}H NMR spectroscopy and GPC. Subsequently, P3OT-*b*-PDMS diBCPs with different block length ratios were

obtained via Cu-catalyzed azide-alkyne cycloaddition (see Scheme 1: P3OT$_{26}$-*b*-PDMS$_{12}$, P3OT$_{26}$-*b*-PDMS$_{50}$, P3OT$_{26}$-*b*-PDMS$_{138}$, where the subscripts specify the number-average degree of polymerization), purified from homopolymer contaminants by repeated preparative size exclusion chromatography, and isolated by precipitation into methanol. The purple diBCPs, which were solid in the case of 32 and 66 mol% PDMS content (P3OT$_{26}$-*b*-PDMS$_{12}$ and P3OT$_{26}$-*b*-PDMS$_{50}$), and soft gums in the case of 84 mol% PDMS content (P3OT$_{26}$-*b*-PDMS$_{138}$), were obtained in an isolated yield of max. 33%. The block ratios of the P3OT-*b*-PDMS diBCPs were determined by ^{1}H NMR spectroscopy and the polydispersity indices, by GPC (see Table 1, NMR spectra in Figure S2-S4, and GPC profiles in Figure S5 in the SI).

Table 1. Number-average molecular weights (M_n) and polydispersity indices (PDI) of P3OT homopolymer and P3OT-*b*-PDMS diblock copolymers.

	Block length ratio[a]	M_n [g mol^{-1}][b]	PDI (M_w/M_n)[c]
P3OT$_{26}$	-	5,200	1.07
P3OT$_{26}$-*b*-PDMS$_{12}$	1 : 0.5	6,100	1.19
P3OT$_{26}$-*b*-PDMS$_{50}$	1 : 2	8,800	1.15
P3OT$_{26}$-*b*-PDMS$_{138}$	1 : 5	15,500	1.11

[a]From ^{1}H NMR spectroscopy. [b]The molar mass (M_n) of P3OT homopolymer was determined from MALDI-TOF mass spectroscopy and M_n of the diblock copolymers by combining M_n of the P3OT block obtained by MALDI-TOF mass spectroscopy and the block length ratio obtained by ^{1}H NMR spectroscopy. [c]From GPC analysis relative to polystyrene standards.

2. Characterization of π-conjugation and crystallinity of P3OT-*b*-PDMS diblock copolymers in the bulk state. The degree of π-conjugation and crystallization of the P3OT block of the diBCPs was studied by UV/Vis spectroscopy, wide angle X-ray scattering (WAXS), and differential scanning calorimetry (DSC). The solution-state UV/Vis spectra of the yellow P3OT-*b*-PDMS solutions in THF all exhibit an absorption maximum for π-π* transitions at ca. 445 nm, suggesting a similar conjugation length in these diBCPs (see representative UV/Vis spectra of molecularly dissolved P3OT$_{26}$-*b*-PDMS$_{50}$ in Figure 1c as well as UV/Vis spectra of P3OT$_{26}$-*b*-PDMS$_{12}$ and P3OT$_{26}$-*b*-PDMS$_{138}$ in Figure S6).[94] An absorption maximum at this wavelength is characteristic of regioregular P3OT.[95-97] WAXS was performed on films cast from concentrated THF solutions of the diBCPs (see representative WAXS

patterns in Figure S7). The WAXS patterns exhibited the characteristic peaks at 2θ = 4.4° for the (100) reflection (d ~ 20.1 Å) and 2θ = 8.6-9.3° for the (200) reflection (d ~ 9.5-10.3 Å) which correspond to the reported interlayer d spacing and three-dimensional packing of regioregular P3OT.[95, 98] The (300) reflections, however, were obscured in both patterns due to the broad peak at 2θ = 12.4° which corresponds to the PDMS block, as has previously been observed in WAXS studies of P3HT-*b*-PDMS diBCPs.[41] The weak diffraction peak at 2θ = 23.4-23.7° corresponds to a d spacing of 3.8 Å and was assigned to the stacking distance of thiophene rings between two polymer chains. This indicates that the regioregular P3OT chains self-organize into a 3D structure comprised of crystalline lamellar ordering.[95] The crystallization of the P3OT block was further investigated by DSC and is discussed in Figure S8 (see SI). The DSC measurements confirmed that the diBCPs possess a regioregular, semicrystalline P3OT block and revealed that their crystallization behaviour is only slightly influenced by the length of the PDMS coblock.

3. Solution self-assembly of P3OT-*b*-PDMS; formation of polydisperse, multi-micron-long fibers.

The solution self-assembly of P3OT-*b*-PDMS diBCPs with three different P3OT/PDMS block ratios of 1:0.5 ($P3OT_{26}$-*b*-$PDMS_{12}$,), 1:2 ($P3OT_{26}$-*b*-$PDMS_{50}$), and 1:5 ($P3OT_{26}$-*b*-$PDMS_{138}$, see Table 1) was studied by heating a preweighed amount of the respective diBCP in decane (a selective solvent for PDMS) to 100°C for 2 h, followed by slowly cooling the solution to room temperature and aging for several days. Upon heating to 100°C, the polymer dissolved and the solution became yellow to yellow-orange. After cooling the solution to room temperature and aging, the polymer dispersion turned purple.

For analysis by bright field transmission electron microscopy (TEM) an aliquot of the polymer solution was drop cast onto a carbon-coated copper TEM grid and the solvent was allowed to evaporate at room temperature before imaging. The formation of fiber-like micelles was observed and, due to the dense packing of the P3OT chains, the micelle cores appear dark in bright field TEM images even in the absence of staining. $P3OT_{26}$-*b*-$PDMS_{50}$ and $P3OT_{26}$-*b*-$PDMS_{138}$ with block length ratios of 1:2 and 1:5, respectively, formed fiber-like micelles up to a few microns in length (see Figure S9a and S9b). For $P3OT_{26}$-*b*-$PDMS_{12}$, with a block length ratio of 1:0.5, the formation of fiber-like micelles with lengths

up to a few micrometers was also observed but these formed aggregates on the carbon coated TEM grids and the dimensions of individual micelles could not be determined (see Figure S9c). In addition, P3OT$_{26}$-*b*-PDMS$_{12}$ diBCP micelles tend to precipitate after ca. 4-5 months, although these are redispersible on shaking. This lack of long term colloidal stability was not observed for P3OT$_{26}$-*b*-PDMS$_{50}$ and P3OT$_{26}$-*b*-PDMS$_{138}$ diBCP micelle solutions in decane, which were found to be colloidally stable for >5 months in the same solvent without any signs of precipitation. This suggests that the shorter PDMS block length of the P3OT$_{26}$-*b*-PDMS$_{12}$ diBCP is not sufficient to stabilize the polymer fibers against aggregation. Since a statistical analysis of P3OT$_{26}$-*b*-PDMS$_{12}$ micelle lengths by TEM was not possible due to severe micelle aggregation, we focused on studying the growth of fiber-like micelles that formed from P3OT$_{26}$-*b*-PDMS$_{50}$ and P3OT$_{26}$-*b*-PDMS$_{138}$ diBCPs.

The structural features of the fiber-like micelles were probed for the case of the P3OT$_{26}$-*b*-PDMS$_{50}$ diBCP. TEM analysis of these fiber-like micelles revealed uniform widths of ca. 13 ± 2 nm (see Figure S10). The width agrees with the theoretically expected width of 10.4 nm for a core structure consisting of fully extended P3OT$_{26}$ chains (length of monomer unit = 0.4 nm).[43, 99] This is consistent with previous work on P3AT homopolymers where it has been shown that polymers with a degree of polymerization $DP_n < 60$ form nanofiber cores consisting of fully extended chains.[100, 101] The P3AT chains pack in a face-to-face fashion, perpendicular to the growing direction of the polymer fiber through intermolecular π-π interactions.[86-88, 102] The height of the P3OT$_{26}$-*b*-PDMS$_{50}$ micelles was found to be ca. 3.7 nm by AFM (see representative AFM height image of P3OT$_{26}$-*b*-PDMS$_{50}$ micelles and corresponding height profiles in Figure 1a and b, as well as Figure S11) and suggested an overall tape-like shape for the P3OT cores. As a d spacing of 1.86 nm has been found for crystalline P3OT domains,[103] the P3OT-*b*-PDMS micelles consist of 2 vertical stacks of the diBCP (see Figure 2).

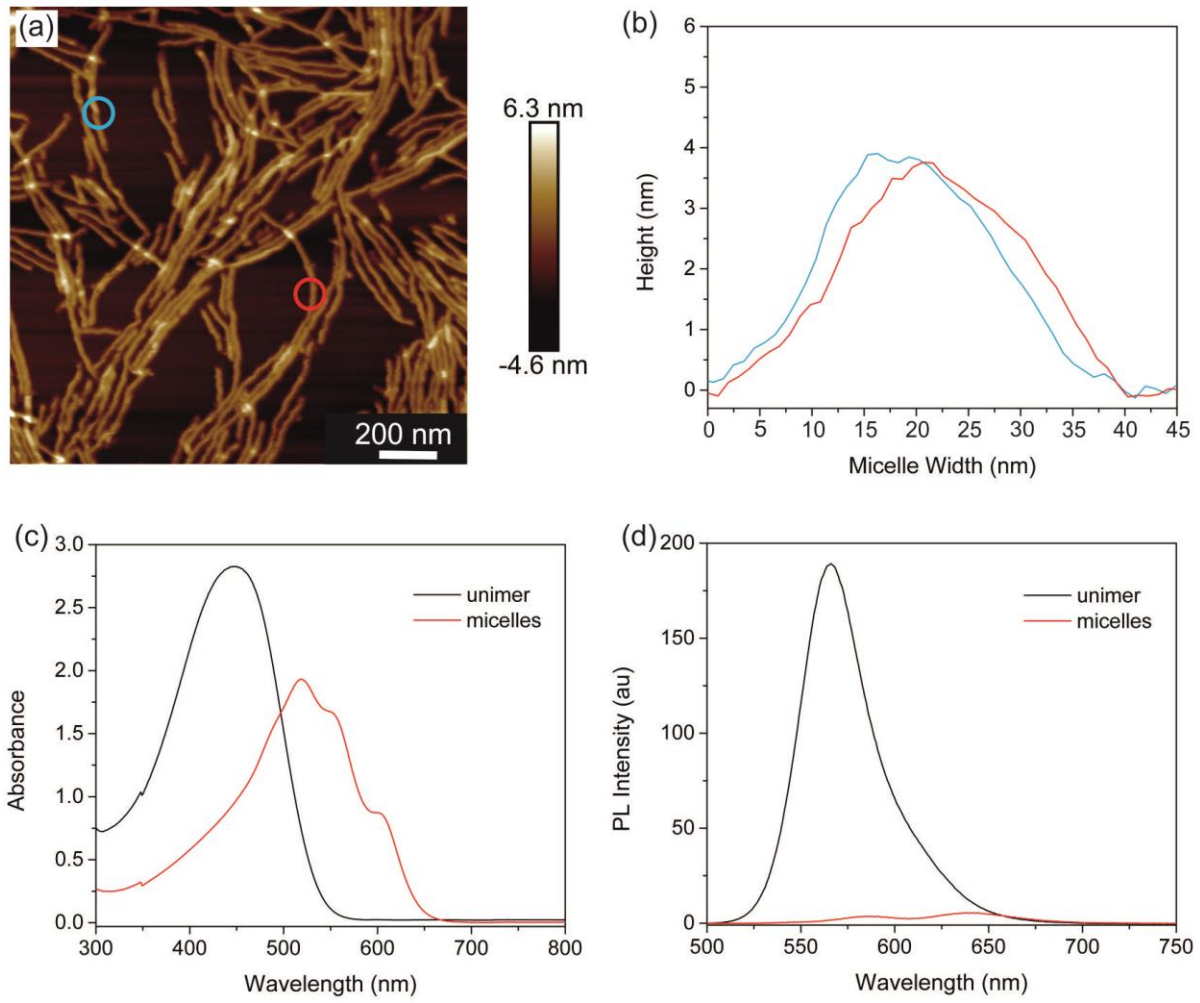

Figure 1. (a) AFM height image of polydisperse, multi-micron-long fiber-like P3OT$_{26}$-*b*-PDMS$_{50}$ micelles drop-cast from decane and dried for 1 day. (b) Representative height profiles of P3OT$_{26}$-*b*-PDMS$_{50}$ micelles taken from the blue and the red circles in the AFM height image (a). Further height profiles are illustrated in Figure S11 in the SI. (c) Solution-state UV/Vis spectra of P3OT$_{26}$-*b*-PDMS$_{50}$ unimers (0.1 mg mL^{-1} in THF, black) and micelles (0.1 mg mL^{-1} in decane, red); (d) Solution PL spectra of P3OT$_{26}$-*b*-PDMS$_{50}$ unimers (0.3 mg mL^{-1} in THF, black) and micelles (0.3 mg mL^{-1} in decane, red).

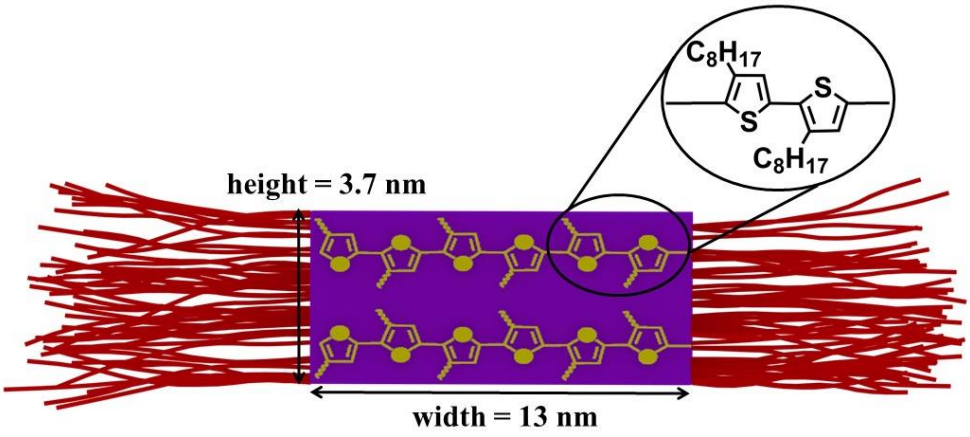

Figure 2. Schematic representation of a cross-section of the crystalline P3OT-*b*-PDMS micelle core which exhibits a tape-like shape.

The crystallinity of the P3OT core in the fiber-like micelles was investigated by UV/Vis spectroscopy, photoluminescence (PL) spectroscopy and WAXS. As these results do not differ significantly for the studied diBCPs, only results obtained for P3OT$_{26}$-*b*-PDMS$_{50}$ are shown (see Figure S6 for more details on P3OT$_{26}$-*b*-PDMS$_{12}$ and P3OT$_{26}$-*b*-PDMS$_{138}$ diBCPs). A representative UV/Vis spectrum of the P3OT$_{26}$-*b*-PDMS$_{50}$ micelle solution in decane is shown in Figure 1c. The spectrum exhibits an absorption maximum at 518 nm, which is significantly red-shifted compared to the corresponding diBCP solution in THF (λ_{max} = 445 nm). The absorption band at ca. 600 nm suggests a crystalline ordering in the P3OT core, which results from strong intermolecular interactions among P3OT chains.[104] Representative photoluminescence (PL) spectra of a P3OT$_{26}$-*b*-PDMS$_{50}$ unimer solution in THF and a micelle solution in decane, both at the same concentration, reveals a negligible emission intensity for the latter compared to the former (Figure 1d). This behaviour is well known for micelles formed from P3HT-containing diBCPs,[39, 41, 42] and indicates fluorescence quenching due to aggregation of polythiophene chains.[105] The absence of a peak at ca. 445 nm in the UV/Vis spectrum of the micelle solution and the significant reduction of the emission intensity observed for the micelle solution compared to the unimer solution indicate that no significant amounts of molecularly dissolved unimer remain in solution.

The crystallinity of the P3OT micellar cores was also studied by WAXS analysis. A representative WAXS pattern of a P3OT$_{26}$-*b*-PDMS$_{50}$ micelle film cast from a micelle solution in decane is illustrated in Figure S12. The WAXS pattern is similar to that observed for the corresponding P3OT$_{26}$-*b*-PDMS$_{50}$ diBCP film cast from the polymer solution in THF (see Figure S7). Both WAXS patterns exhibit the characteristic peaks at 2θ = 4.4° for the (100) reflection (d ~ 20.1 Å) and 2θ = 8.6° for the (200) reflection (d ~ 10.3 Å) corresponding to the three-dimensional packing of the regioregular P3OT polymer chains. This indicates that the fiber-like micelles consist of crystalline cores as suggested by the UV/Vis data.[95, 98] Similar to the WAXS pattern for the diBCP film cast from the polymer solution in THF, the (300) reflection for the micelle film was obscured due to the broad peak at 2θ = 12.4° which corresponds to an amorphous halo for the PDMS block. The WAXS pattern collected from a P3OT$_{26}$-*b*-PDMS$_{12}$ micelle film, however, does not exhibit a broad and intense PDMS peak at 2θ = 12.4° and the (300) reflection at 2θ = 13.6° (d ~ 6.5 Å) is clearly visible (see Figure S12).

4. Living CDSA of P3OT$_{26}$-*b*-PDMS$_{50}$ and P3OT$_{26}$-*b*-PDMS$_{138}$. Seed micelles of P3OT-*b*-PDMS were prepared from solutions of the polydisperse, multi-micrometer long fiber-like P3OT$_{26}$-*b*-PDMS$_{50}$ and P3OT$_{26}$-*b*-PDMS$_{138}$ micelles in decane described in the previous section by sonication. Moderate sonication (160 W) in a water bath at 22°C for 30 min led to the formation of relatively small seed micelles with average contour lengths of ca. 80 nm in each case (see Figure S13) following a previous protocol.[42] Initial seeded growth experiments were conducted by addition of P3OT-*b*-PDMS unimers as 10 mg mL^{-1} THF solutions corresponding to a unimer-to-mass ratio of 2.5 to the seed micelles (see Scheme 2). Aliquots were taken after aging the solutions for 24 h and were imaged by TEM in the dry state.

Scheme 2. Schematic illustration of the living CDSA of P3OT-*b*-PDMS diblock copolymers.

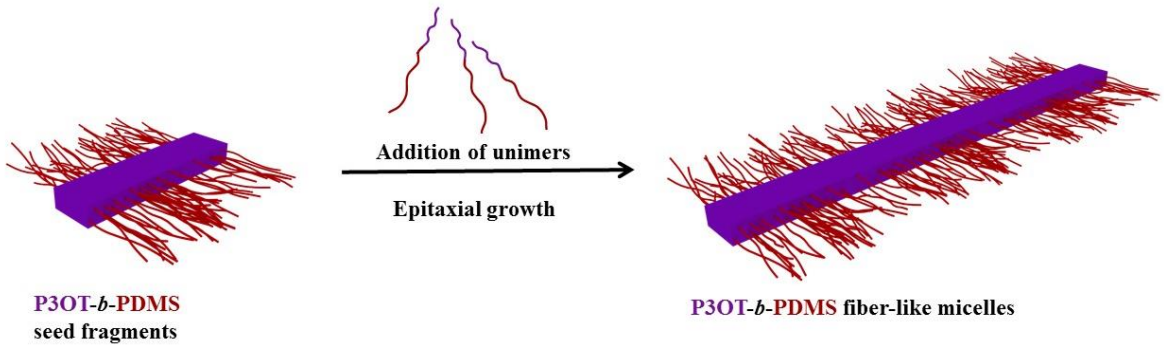

Both sets of seed micelles derived from the P3OT-*b*-PDMS BCPs were found to function as efficient initiators for CDSA. After addition of P3OT$_{26}$-*b*-PDMS$_{50}$ or P3OT$_{26}$-*b*-PDMS$_{138}$ unimers (in THF) to a seed solution (in decane), fiber-like micelles with a number-average length L_n of 282 nm (PDI = 1.12) and 241 nm (PDI = 1.24) were formed (see Figure S14). The L_n of these fiber-like micelles was ca. 98% (P3OT$_{26}$-*b*-PDMS$_{50}$) and 89% (P3OT$_{26}$-*b*-PDMS$_{138}$) of the theoretically predicted micelle length (L_n = 287 nm for P3OT$_{26}$-*b*-PDMS$_{50}$ and L_n = 270 nm for P3OT$_{26}$-*b*-PDMS$_{138}$). This indicates a near quantitative conversion of the added unimer into the micelles for both diBCPs and is consistent with a living CDSA process. The calculation of theoretically predicted micelle length was based on the added BCP unimer to seed mass ratio and assumes quantitative conversion to active seeds by sonication, complete addition of unimer, a constant linear aggregation number of BCP molecules for the grown

micelles, and the absence of micelle growth termination events. The concentration of THF, a common solvent for both blocks of P3OT-*b*-PDMS, was kept well below 1% and thus highly disfavouring the dissolution of the initial seed crystals.

Encouraged by these initial results, seeded growth was investigated in more detail, focusing on the $P3OT_{26}$-*b*-$PDMS_{50}$ diBCP as this material showed a higher efficiency for living CDSA, leading to micelles with a length closer to that predicted theoretically and a lower length polydispersity. To this end, short stub-like seed micelles composed of $P3OT_{26}$-*b*-$PDMS_{50}$ with an average contour length of 36 nm (PDI = 1.14) by TEM were prepared by applying more vigorous sonication using a 100 W ultrasonic processor equipped with a sonotrode for 4 h at 0 °C (see Figure 3).

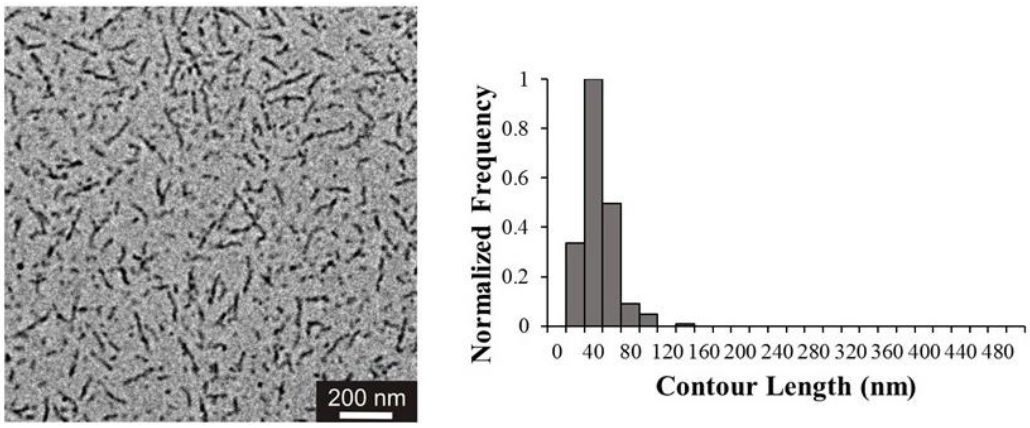

Figure 3. TEM micrograph and corresponding histogram of $P3OT_{26}$-*b*-$PDMS_{50}$ seed micelles (L_n = 36 nm, PDI = 1.14) obtained by sonication of polydisperse, multi-micron-long micelles at 0°C for 4 h in decane.

The seed micelles obtained exhibited a low standard deviation of ca. 13 nm compared to the longer seeds used initially (L_n ca. 80 nm, standard deviation ca. 37 nm), thus facilitating the observation of micelle growth and also promoting the formation of monodisperse micelles by living CDSA. Growth from these small seed micelles in decane was investigated by adding $P3OT_{26}$-*b*-$PDMS_{50}$ unimer as a 10 mg mL^{-1} solution in THF, corresponding to m_{unimer}/m_{seed} values of 2.5, 5, 7.5, 10, 12.5, 15, and 20 (see Figure 4a and Table S1).

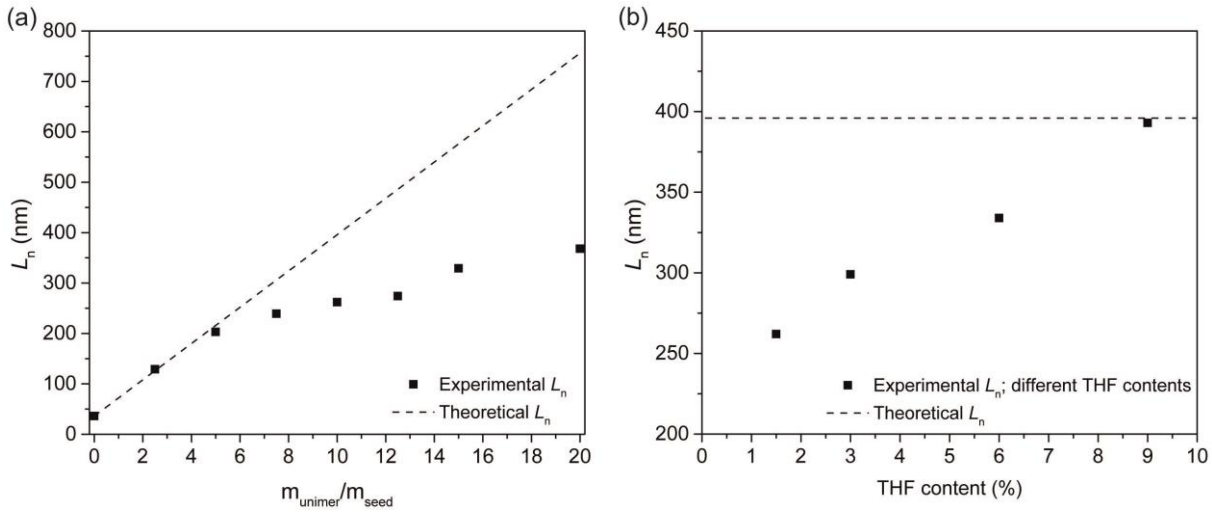

Figure 4. Number-average micelle contour length plotted against unimer-to-seed ratio for the fiber-like P3OT$_{26}$-*b*-PDMS$_{50}$ micelles obtained by adding the respective amount of P3OT$_{26}$-*b*-PDMS$_{50}$ unimer in THF to 6 µg of P3OT$_{26}$-*b*-PDMS$_{50}$ seed micelles in decane at 22°C (a) and by adding 60 µg of P3OT$_{26}$-*b*-PDMS$_{50}$ unimer in THF to 6 µg of P3OT$_{26}$-*b*-PDMS$_{50}$ seed micelles in a decane/THF solvent mixture with varying THF contents at 22°C (b). The solutions were aged for 2 days at 22°C before TEM samples were prepared. Black dashed line: Theoretically predicted micelle lengths based on the mass of seed micelles and added unimer.

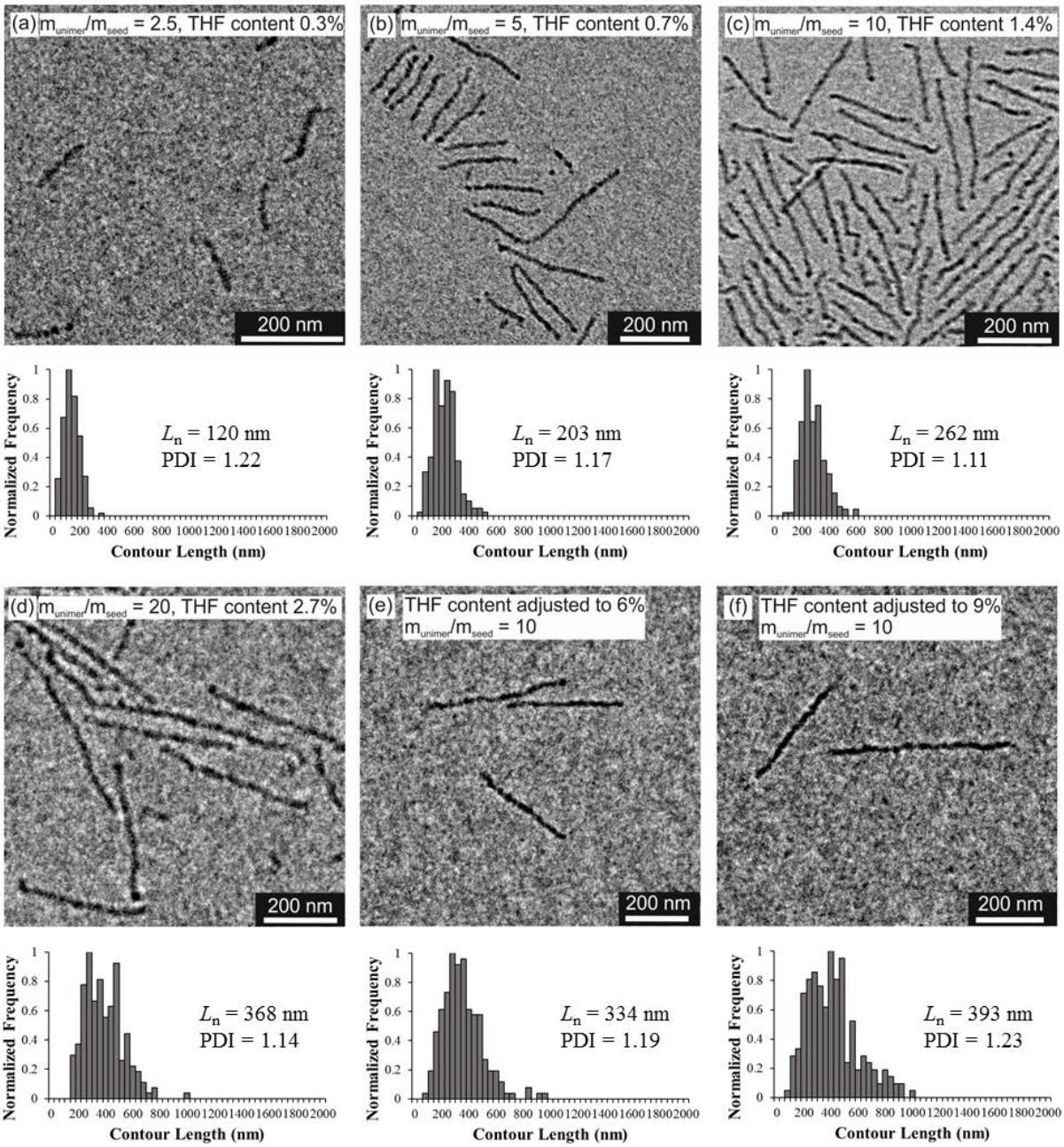

Figure 5. TEM micrographs and corresponding histograms for the fiber-like $P3OT_{26}$-*b*-$PDMS_{50}$ micelles which were obtained from adding 15 µg (a), 30 µg (b), 60 µg (c), and 120 µg (d) $P3OT_{26}$-*b*-$PDMS_{50}$ unimer to 6 µg of $P3OT_{26}$-*b*-$PDMS_{50}$ seed micelles in decane and from adding 60 µg $P3OT_{26}$-*b*-$PDMS_{50}$ unimer to 6 µg of $P3OT_{26}$-*b*-$PDMS_{50}$ seed micelles in a decane/THF solvent mixture with final THF fractions of 6% (e) and 9% (f).

After aging the solutions at room temperature for two days, fiber-like micelles of varying length between L_n 129 nm and 368 nm with moderate length polydispersities (PDI <1.22) formed, as shown by TEM (Figure 5). Adding increasing amounts of unimer to the solution of seed micelles yielded fiber-like micelles with increasing average contour lengths. The best match of measured and theoretically

predicted average micelle lengths was observed for unimer additions corresponding to unimer-to-seed ratios of ≤ 5 and suggest a quantitative conversion of unimer into fibers. This is also qualitatively supported by UV/Vis spectroscopy (see Figure S15) where the spectra of these micelle solutions suggest crystalline ordering in the P3OT core, indicated by the absorption band at ca. 600 nm, and also absence of a peak at 445 nm, indicating that no significant amounts of unimer were left in solution.[104] The fraction of surviving seed micelles was in general well below 10% (see histograms in Figure 5), indicating that growth at the termini of the seed micelles occurs efficiently, at least initially. At unimer-to-seed ratios > 5 longer fiber-like micelles were formed but the difference between measured and theoretically expected micelle length increased substantially (Figure 4a). However, non-converted BCP was not observed for high values of $m_{unimer}/m_{seed} \geq 10$. This may be a consequence of competing homogenous nucleation taking place simultaneously to epitaxial growth from the micelle seeds as the solubility of the polythiophene block in n-alkanes is low, resulting in a rather low overall solubility of the diBCP.

This assumption is supported by a control experiment in which unimer was self-assembled under the same conditions but in the absence of seed micelles. In this experiment a quantity of the $P3OT_{26}$-*b*-$PDMS_{50}$ unimer solution (12 µl of a 10 mg mL^{-1} in THF) corresponding to the highest amount of unimer solution added to seed micelles in Figure 4a was injected into decane, and the resulting colloidal solution aged at room temperature for two days, the same length of time as for the seeded growth experiments. In the absence of seed micelles, formation of polydisperse fibers with contour lengths between 40 nm and >1000 nm and an average contour length of 165 nm (PDI = 1.80) was observed (see Figure S16 in SI). This observation suggests that, the micelles obtained in the analogous seeded growth experiments with moderate length polydispersities of 1.11-1.22 are predominantly formed by epitaxial crystallization at the termini of the seed micelles. The control experiment, however, also shows that it is possible for homogenous nucleation to take place, in particular at high unimer-to-seed ratios of m_{unimer}/m_{seed} = 10-20. Despite this, the largest obtained micelle length of 368 nm and the apparent unimer uptake of 50% when using $P3OT_{26}$-*b*-$PDMS_{50}$ exceeded the self-assembly performance of their P3HT analogs.[41] This suggests that introducing increased solubility and a larger steric barrier into the polythiophene repeat units by using a longer, n-octyl side group instead of an n-hexyl group may slow down the face-to-face packing of the polymer chains which is driven by intermolecular π-π interactions.[86-88, 102] We postulate

that this might favour living CDSA by promoting structural rearrangement of the polythiophene chains and by decreasing the amount of defects during the self-assembly process. Formation of defects due to rapid crystallization could lead to lattice distortion and strain in the crystal growth direction and could explain the low unimer conversion for P3HT-containing diBCPs by rendering the core termini inactive for further epitaxial growth.[39, 41, 42]

Seeded growth experiments were repeated using P3OT$_{26}$-*b*-PDMS$_{138}$ and living CDSA initiated from short stub-like P3OT$_{26}$-*b*-PDMS$_{138}$ seed micelles with an average contour length of 29 nm (PDI = 1.19) was also studied (see Table S2, Figure S17 and Figure S18). Although the measured micelle lengths of up to 358 nm were comparable to those found for analogous seeded growth experiments with P3OT$_{26}$-*b*-PDMS$_{50}$, the length polydispersity of <1.39 observed for micelles formed from P3OT$_{26}$-*b*-PDMS$_{138}$ was found to be significantly larger than that obtained when using P3OT$_{26}$-*b*-PDMS$_{50}$ (PDI ≤ 1.22). This increased length polydispersity for the case of P3OT$_{26}$-*b*-PDMS$_{138}$ might be due to the increased steric barrier associated with the longer PDMS corona. Based on previous studies of micelle growth kinetics, this would be expected to lead to a slower rate of seeded growth and therefore to increased competition from the formation of new micelles by homogenous nucleation.[106]

5. Living CDSA of P3OT$_{26}$-*b*-PDMS$_{50}$ at varied concentration of common solvent. By performing the seeded growth experiments in the presence of an increased fraction of common solvent homogenous nucleation is suppressed, as demonstrated by the previous study with P3HT-*b*-P2VP in isopropanol with added THF.[39] In addition, it is likely that structural rearrangement of the core-forming P3OT chains leading to a more regular packing and a reduction of defects might be promoted under analogous conditions. The THF volume fraction was kept below 10% as the L_n of seed micelles increased in length in decane/THF solvent mixtures with THF volume fractions >10% after aging for two days without further addition of unimer (see data for control experiments in Table S3). This suggests that solvent-induced self-seeding occurs under these conditions. Thus, seeded growth experiments with a unimer-to-seed ratio of 10, for which the length of the obtained micelles and the theoretically expected micelle length differed by ca. 30%, were repeated in the presence of an increased amount of THF, with final

THF volume fractions of 3%, 6%, and 9% compared to 1.5%. The fraction of common solvent of the decane/THF solvent mixture was increased by adding the desired amount of THF before the addition of unimer in the same solvent. Fiber-like micelles with average contour lengths of 299 nm, 334 nm, and 393 nm with length polydispersities of 1.16-1.23 were obtained in the presence of THF fractions of 3, 6 and 9%, respectively, significantly exceeding the micelle lengths of L_n = 262 nm (PDI = 1.11) obtained in the presence of 1.5% THF and, in the case of using a THF fraction of 9%, closely matching the theoretically predicted length L_n of 396 nm (see Figure 4b, Figure 5e and f and Table S1).

Clearly an increased amount of THF favours micelle growth and it is likely that under these conditions more defect-free crystalline domains are being formed. However, after aging the micelle solutions with THF fractions of 6 and 9% significant amounts of unimer were still present in the micelle solutions for several weeks according to UV/Vis spectroscopy (see Figure 6). That the presence of certain amounts of common solvent for both blocks promotes micelle growth is also evident when further increasing the amount of unimer at a final THF volume fraction of 9% (e.g. m_{unimer}/m_{seed} = 25: L_n = 503 nm and PDI = 1.25; see Figure S19). In a control experiment an identical amount of $P3OT_{26}$-*b*-$PDMS_{50}$ unimer solution was injected into a decane/THF solvent mixture consisting of a total THF fraction of 9 vol% in the absence of seed micelles. After aging at room temperature for two days this gave fibers with L_n = 339 nm with a significantly larger dispersity (PDI = 1.44) suggesting that at higher values of m_{unimer}/m_{seed} homogenous nucleation can still occur (see Figure S20).

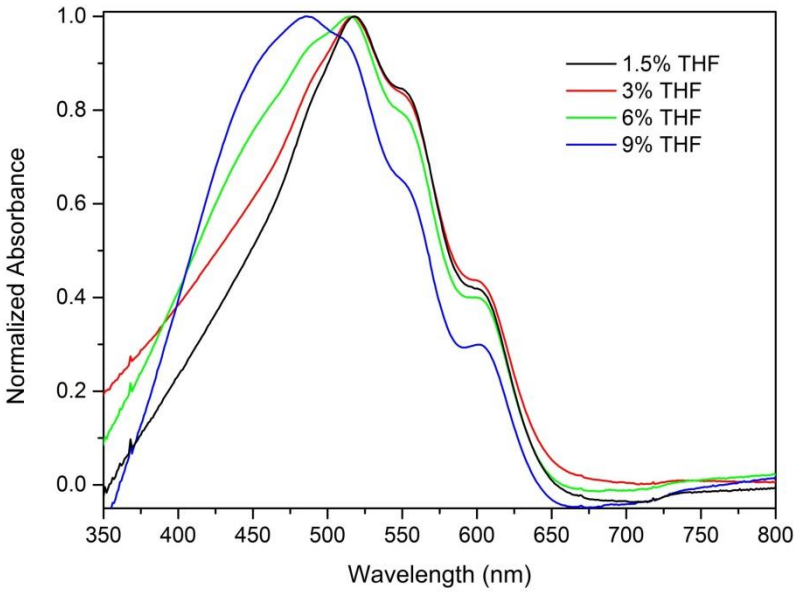

Figure 6. UV/Vis spectra of micelle solutions obtained from adding 60 µg P3OT$_{26}$-*b*-PDMS$_{50}$ unimer to 6 µg of P3OT$_{26}$-*b*-PDMS$_{50}$ seed micelles in a decane/THF solvent mixture with final THF fractions of 1.5%, 3%, 6%, and 9% at 22°C, micelle solutions aged at 22°C for at least two days before samples were prepared for analysis.

Sonication might be expected to introduce defects into the seed micelles and to therefore hinder growth even in early stages of their elongation on addition of unimer. For this study, vigorous sonication at 0°C over 4 h was applied to produce uniform, small seed micelles, which represents harsher conditions than those previously reported for polythiophene-containing diBCP fiber-like micelles.[39, 41, 42] However, comparison of GPC traces of a P3OT$_{26}$-*b*-PDMS$_{50}$ unimer solution in THF and of a corresponding solution in THF prepared by redissolving seed fragments in THF were very similar and showed no evidence for chain scission induced by sonication (Figure S21). However, the introduction of ultrasound-induced changes to the internal structure of the P3OT core could not be ruled out. We therefore performed an additional control experiment in which seed fragments were prepared without the use of sonication but under conditions that should promote homogenous nucleation instead.[107] This was achieved by the addition of small amounts of unimer as a 10 mg mL^{-1} THF solution to decane at 0°C with the fraction of common solvent for both blocks kept well below 1%. This procedure afforded seed micelles with L_n = 47 nm (PDI = 1.21, see Figure S22a) that did not grow further over 3 days. Using these seed micelles for seeded growth experiments by adding unimer corresponding to a unimer-to-seed ratio of 10 and using THF fractions of 1.5, 6 and 9%, micelles with average contour lengths of 229 nm (PDI = 1.18), 281 nm (PDI = 1.20), and 376 nm (PDI = 1.22) were obtained (see Figure S22).

These lengths are similar to those obtained when initiating growth from seed micelles prepared by sonication under analogous conditions (see Table S1, entries 1-4, 1-9, and 1-10), which suggests that sonication of micelles does not introduce additional defects in the core that influence subsequent epitaxial growth from the seeds.

6. Living CDSA of P3OT$_{26}$-*b*-PDMS$_{50}$ under varied temperature and solvent conditions. In order to optimize conditions for the living CDSA of P3OT$_{26}$-*b*-PDMS$_{50}$ diBCPs, seeded growth experiments were performed at 10°C, 35°C and 40°C.[89] Seeded growth experiments were carried out at a unimer-to-seed ratio of 10 where, at room temperature, the measured micelle length deviated from the theoretically predicted micelle length by ca. 30%. Figure 7 shows a comparison of micelles formed upon adding unimer in THF corresponding to m_{unimer}/m_{seed} = 10 to seed micelles with an average contour length (L_n) of 36 nm (PDI = 1.14) in decane at 10°C, 22°C, 35°C, and 40°C, respectively, followed by aging the micelle solution at the respective temperature for 2 days. At 10°C, an average length L_n = 41 nm (PDI = 1.48) was determined while at 22°C, under otherwise identical conditions, micelles with L_n = 262 nm (PDI = 1.11) were formed, suggesting that micelle elongation is highly disfavoured at lower temperatures. Interestingly, on increasing the temperature to 35°C and 40°C and keeping all other parameters constant, micelle growth was improved and fiber-like micelles with an average length of 330 nm (PDI = 1.21) and 434 nm (PDI = 1.24) were obtained, respectively (see Figure 7).

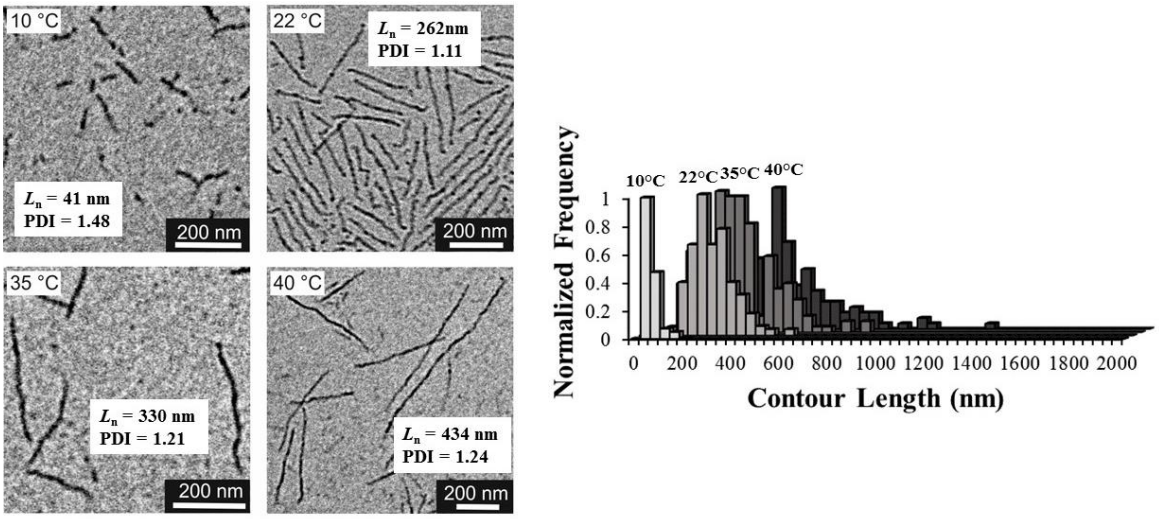

Figure 7. Effect of temperature on P3OT-*b*-PDMS fiber length by seeded growth. Micelles were obtained from adding 60 µg $P3OT_{26}$-*b*-$PDMS_{50}$ unimer in THF to 6 µg of $P3OT_{26}$-*b*-$PDMS_{50}$ seed micelles (L_n = 36 nm, PDI = 1.14) in decane at 10°C, 22°C, 35°C and 40°C, aged at the respective temperature for two days. TEM micrographs for the fiber-like $P3OT_{26}$-*b*-$PDMS_{50}$ micelles obtained at the respective temperature (left) and corresponding histograms of the contour length distribution of samples (right; increasing temperature from left to right). The theoretically predicted micelle length is 396 nm.

The substantial increase in PDI for the fibers formed at 10°C compared to the seeds (1.48 vs 1.14) indicates that homogenous nucleation is strongly favoured at a lower temperature, presumably due to the lower solubility of the polymer. The length obtained at 35°C of 330 nm differs from the theoretically expected micelle length of 396 nm by less than 17%, suggesting a more efficient micelle growth at elevated temperature than at room temperature under otherwise identical conditions. An increase in temperature may promote structural rearrangement and thus more regular packing of P3OT chains via local annealing steps which could promote growth by avoiding the formation of defects. In addition, an increased temperature is expected to improve the solvent quality which would disfavour homogenous nucleation thereby leading to the growth of longer micelles.[89] The average length obtained at 40°C actually exceeded the theoretically predicted micelle length by ca. 10%. We speculate that the increased solvent quality of the diBCP in decane at 40°C may lead to partial dissolution of the initial seeds before unimer was added (see discussion in the SI). This would lead to an underestimation of the theoretically calculated micelle length.

Seeded growth experiments were also conducted at 35°C in the presence of increasing amounts of unimer (Figure 8a). By adding increasing amounts of unimer as a 10 mg mL^{-1} solution in THF (m_{unimer}/m_{seed} = 5, 7.5, 10, 12.5, 15, 20, and 25) to a solution of seed micelles in decane at 35°C and aging the solutions for 2 days, micelles with an increased average contour length of up to 572 nm (PDI = 1.22) were obtained, the highest value to date for polythiophene-based micelles by seeded growth (see Figure 8a and Figure S23).

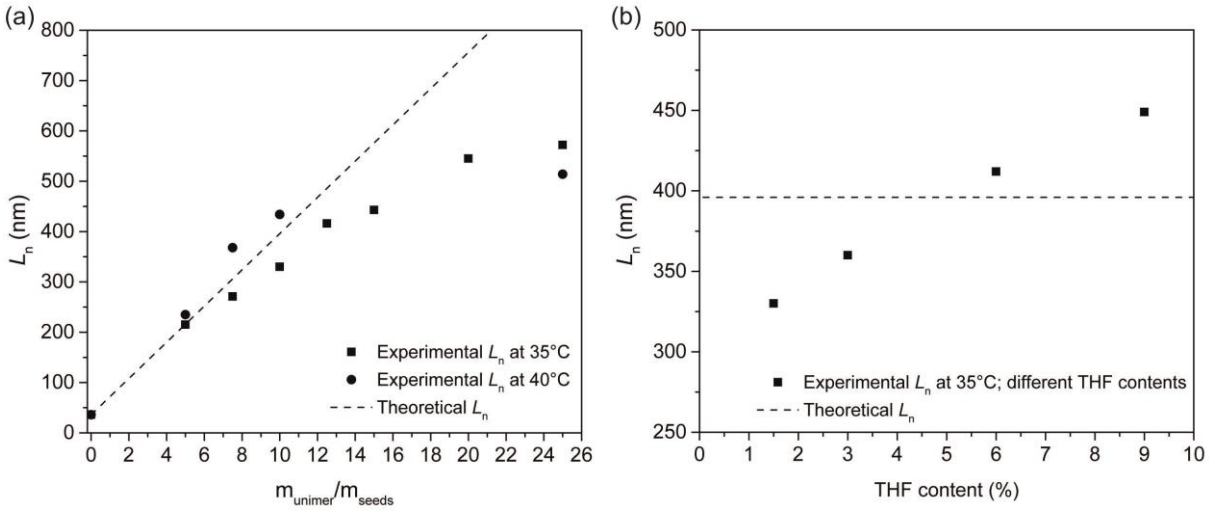

Figure 8. Number average micelle contour length plotted against unimer-to-seed ratio for the fiber-like $P3OT_{26}$-*b*-$PDMS_{50}$ micelles obtained by adding the respective amount of $P3OT_{26}$-*b*-$PDMS_{50}$ unimer in THF to 6 µg of $P3OT_{26}$-*b*-$PDMS_{50}$ seed micelles in decane at 35°C (a, black squares) and 40°C (a, black circles), and by adding 60 µg of $P3OT_{26}$-*b*-$PDMS_{50}$ unimer in THF to 6 µg of $P3OT_{26}$-*b*-$PDMS_{50}$ seed micelles in a decane/THF solvent mixture with varying THF contents at 35°C (b). Black dashed line: Theoretically predicted micelle lengths based on the mass of seed micelles and added unimer.

At a unimer-to-seed ratio of ≤ 12.5, the discrepancy for measured and theoretically expected micelle lengths in 35°C seeded growth experiments was less than 15%. For a unimer-to-seed ratio of 15, the measured micelle length drops to ca. 80% of the theoretically expected micelle length and thus substantial amounts of residual unimer in solution were expected. This is consistent with UV/Vis spectroscopic data where a significant shoulder is observed at ca. 440-450 nm (see Figure S24). For seeded growth experiments up to a unimer-to-seed ratio of 10 molecularly dissolved diBCP was not detected by UV/Vis spectroscopy (Figure S24).

Significantly, for unimer-to-seed ratios ≥ 15 the shoulder in the UV/Vis spectra at 440-450 nm assigned to molecularly dissolved diBCP was no longer detected. This suggests that for $m_{unimer}/m_{seed} \geq 15$, homogenous nucleation may take place in addition to seeded growth (Figure S24). This phenomenon has already been suggested to occur at room temperature but at a considerably earlier stage of growth ($m_{unimer}/m_{seed} = 10$). This indicates that at an increased temperature of 35°C homogenous nucleation is disfavoured due to an increased solvency of the P3OT block. Keeping the unimer-to-seed ratio constant at $m_{unimer}/m_{seed} = 10$ and only increasing the amount of common solvent from 1.5% to 3%, 6%, and 9%, thus increasing the solvent quality of the polymer and possibly reducing defects in the micelle cores, leads to a growth of longer micelles with average contour lengths of 360 nm (PDI = 1.31), 412 nm (PDI = 1.21), and 449 nm (PDI = 1.35) in the presence of 3%, 6% and 9% THF, respectively, compared to an average micelle length of 330 nm (PDI = 1.21) obtained at 35°C in the presence of 1.5% THF (see Figure 8b and Figure S25). A trend of increasing micelle length with increasing THF fraction was previously noted at 22°C, but in contrast to that case, significant amounts of unimer remained in solution when performing seeded growth experiments at 35°C, in particular in the presence of 9% THF (see UV/Vis spectra in Figure S26 in SI). The presence of significant amounts of unimer, the PDI increase, and the formation of micelles above the theoretical length under the latter conditions suggests that dissolution of micellar domains with lower crystallinity or partial seed dissolution may take place to a certain extent. Control over micelle growth is therefore limited under these conditions. A further consideration is that although the P3OT BCP has a narrow molar mass distribution, it is not monodisperse. It is therefore likely that residual unimer consists of material in which the P3OT block is slightly shorter and the corona-forming PDMS block is slightly longer making the polymer chains intrinsically more soluble.

7. General aspects of living CDSA at elevated temperature and in the presence of increased fractions of common solvent. To extend the scope of the new protocol involving the use of elevated temperature and the presence of increased amounts of THF for seeded growth experiments, we also investigated seeded growth behavior of $P3OT_{20}$-*b*-PS_{60} (characterization data shown in Figure S30 and

S31) at 22°C and 35°C in the presence of different THF fractions. P3OT$_{20}$-*b*-PS$_{60}$ unimer as a 10 mg mL^{-1} solution in THF was added to P3OT$_{20}$-*b*-PS$_{60}$ seed micelles with an average length L_n = 40 nm (PDI = 1.09, see Figure S32) in butyl acetate prepared by sonicating a solution of polydisperse, multi-micron-long fiber-like P3OT$_{20}$-*b*-PS$_{60}$ micelles for 4 h at 0°C. The average contour length L_n obtained at 22°C and 35°C when using a unimer-to-seed ratio of 10 was 120 nm (PDI = 1.20) and 358 nm (PDI = 1.16), respectively (see Table S4 and Figure S33). This reveals that an increased temperature of 35°C significantly favours micelle growth and is in accordance with the trend observed for the living CDSA of P3OT-*b*-PDMS diBCPs. In addition, when increasing both the temperature and the THF fraction, a further increase of micelle length was observed, in line with what is expected based on analogous experiments with P3OT-*b*-PDMS. By keeping the unimer-to-seed ratio at 10 and only increasing the THF fraction to 9%, micelle lengths L_n of 198 nm (PDI = 1.16) and 537 nm (PDI = 1.25) were obtained at 22°C and 35°C, respectively (see example TEM images in Figure S33). Again this demonstrates that performing seeded growth experiments with diBCPs containing a polythiophene block in the presence of an elevated temperature combined with significant amounts of common solvent promotes micelle growth. The micelle length (537 nm) detected for a unimer-to-seed ratio of 10 at 35°C exceeded that expected theoretically (440 nm). As with the case of P3OT-*b*-PDMS, this is probably due to dissolution of micelle regions with lower crystallinity under these conditions, as previously suggested for P3OT-*b*-PDMS.

8. Summary

P3OT-*b*-PDMS diBCPs with a regioregular, crystallizable π-conjugated P3OT core-forming segment and different block length ratios of ca. P3OT:PDMS = 1:0.5, 1:2, and 1:5 (keeping the P3OT block length constant) were synthesized by Cu-catalyzed azide-alkyne cycloaddition reactions of alkyne-terminated P3OT and azide-terminated PDMS homopolymers. Fiber-like, multi-micron-long micelles with a crystalline, tape-like P3OT core and a PDMS corona were obtained via the solution self-assembly in decane (a selective solvent for the PDMS block). The structural features were determined by TEM and AFM and the crystalline nature of the π-conjugated core was confirmed by UV/Vis and fluorescence

spectroscopy as well as WAXS analysis. The colloidal stability was dependent on the P3OT/PDMS block ratio and, due to the severe aggregation of P3OT$_{26}$-*b*-PDMS$_{12}$ micelles, seeded growth experiments were only performed with P3OT$_{26}$-*b*-PDMS$_{50}$ and P3OT$_{26}$-*b*-PDMS$_{138}$ diBCPs (block ratios of ca. 1:2 and 1:5). The use of elevated temperature and significant concentrations of common solvent (THF) during the self-assembly led to the formation of fiber-like micelles with controlled lengths up to ca. 600 nm (PDI = 1.1-1.3) while suppressing potentially competitive homogenous nucleation. This is significantly longer than those accessible using P3HT BCPs (ca. 250 - 300 nm)[39, 41] suggesting that the presence of a more sterically demanding and solubilising n-octyl substituent promotes seeded growth. We suggest that under the conditions of elevated temperature and significant concentrations of common solvent regular, defect-free packing of core-forming P3OT chains is favored, facilitating epitaxial elongation. This was also demonstrated for the case of the self-assembly of P3OT-*b*-PS, indicating that this protocol facilitates effective length control of fiber-like micelles for other polythiophene-containing diBCPs. The application of these concepts to other BCPs with crystalline core-forming blocks where the formation of long fibers by seeded growth has been problematic will be the subject of future work.[89]

Acknowledgement

U.T. thanks the Humboldt foundation for a Feodor Lynen Research Fellowship.

AUTHOR INFORMATION

Corresponding Author

*E-mail: ian.manners@bristol.ac.uk (I.M.).

Present address

U.T: Advanced Materials and Systems Research, BASF SE, 67056 Ludwigshafen am Rhein, Germany.

Supporting Information. Synthesis and characterization of P3OT$_{26}$-*b*-PDMS$_{12}$, P3OT$_{26}$-*b*-PDMS$_{50}$, P3OT$_{26}$-*b*-PDMS$_{138}$, and P3OT$_{20}$-*b*-PS$_{60}$. Preparation of block copolymer seeds and micelles. Additional experimental data and discussion of results.

References

1. Agbolaghi, S.; Zenoozi, S.; Abbasi, F. Conductive poly(3-hexylthiophene) nanofibers and single crystals covered by coily dielectric oligomers and distinctions between their structures developed by self-seeding and isothermal approaches. *J. Iran. Chem. Soc.* **2018,** 15 (2), 381-398.

2. Sun, S.; Salim, T.; Wong, L. H.; Foo, Y. L.; Boey, F.; Lam, Y. M. A new insight into controlling poly(3-hexylthiophene) nanofiber growth through a mixed-solvent approach for organic photovoltaics applications. *J. Mater. Chem.* **2011,** 21 (2), 377-386.

3. Moulé, A. J.; Meerholz, K. Morphology Control in Solution-Processed Bulk-Heterojunction Solar Cell Mixtures. *Adv. Funct. Mater.* **2009,** 19 (19), 3028-3036.

4. Dennler, G.; Scharber, M. C.; Brabec, C. J. Polymer-Fullerene Bulk-Heterojunction Solar Cells. *Adv. Mater.* **2009,** 21 (13), 1323-1338.

5. Li, G.; Shrotriya, V.; Huang, J.; Yao, Y.; Moriarty, T.; Emery, K.; Yang, Y. High-efficiency solution processable polymer photovoltaic cells by self-organization of polymer blends. *Nat. Mater.* **2005,** 4 (11), 864-868.

6. Perepichka, F. I.; Perepichka, D. F., *Handbook of Thiophene-Based Materials: Applications in Organic Electronics and Photonics*. Wiley: Chichester, 2009.

7. Berson, S.; De Bettignies, R.; Bailly, S.; Guillerez, S. Poly(3-hexylthiophene) Fibers for Photovoltaic Applications. *Adv. Funct. Mater.* **2007,** 17 (8), 1377-1384.

8. Jo, J.; Kim, S.-S.; Na, S.-I.; Yu, B.-K.; Kim, D.-Y. Time-Dependent Morphology Evolution by Annealing Processes on Polymer:Fullerene Blend Solar Cells. *Adv. Funct. Mater.* **2009,** 19 (6), 866-874.

9. Ewbank, P. C.; Laird, D.; McCullough, R. D., *Organic Photovoltaics: Materials, Device Physics, and Manufacturing Technologies*. Wiley-VCH: Weinheim, 2008.

10. Tritschler, U.; Pearce, S.; Gwyther, J.; Whittell, G. R.; Manners, I. 50th Anniversary Perspective: Functional Nanoparticles from the Solution Self-Assembly of Block Copolymers. *Macromolecules* **2017,** 50 (9), 3439-3463.

11. Mai, Y.; Eisenberg, A. Self-assembly of block copolymers. *Chem. Soc. Rev.* **2012,** 41 (18), 5969-5985.

12. Hayward, R. C.; Pochan, D. J. Tailored Assemblies of Block Copolymers in Solution: It Is All about the Process. *Macromolecules* **2010,** 43 (8), 3577-3584.

13. Hamley, I., *Block Copolymers in Solution: Fundamentals and Applications*. Wiley: Chichester, 2005.

14. Gohy, J.-F. Block Copolymer Micelles. *Adv. Polym. Sci.* **2005,** 190, 65-136.

15. Hamley, I. W. Nanotechnology with Soft Materials. *Angew. Chem., Int. Ed.* **2003,** 42 (15), 1692-1712.

16. Hadjichristidis, N.; Pispas, S.; Floudas, G., *Block Copolymers: Synthetic Strategies, Physical Properties, and Applications*. Wiley: Hoboken, 2002.

17. Cameron, N. S.; Corbierre, M. K.; Eisenberg, A. 1998 E.W.R. Steacie Award Lecture Asymmetric amphiphilic block copolymers in solution: a morphological wonderland. *Can. J. Chem.* **1999,** 77 (8), 1311-1326.

18. Cui, H.; Chen, Z.; Wooley, K. L.; Pochan, D. J. Origins of toroidal micelle formation through charged triblock copolymer self-assembly. *Soft Matter* **2009,** 5 (6), 1269-1278.

19. Riess, G. Micellization of block copolymers. *Prog. Polym. Sci.* **2003,** 28 (7), 1107-1170.

20. Jain, S.; Bates, F. S. On the Origins of Morphological Complexity in Block Copolymer Surfactants. *Science* **2003,** 300 (5618), 460-464.

21. Discher, D. E.; Eisenberg, A. Polymer Vesicles. *Science* **2002,** 297 (5583), 967-973.

22. Won, Y.-Y.; Davis, H. T.; Bates, F. S. Giant Wormlike Rubber Micelles. *Science* **1999,** 283 (5404), 960-963.

23. Hailes, R. L. N.; Oliver, A. M.; Gwyther, J.; Whittell, G. R.; Manners, I. Polyferrocenylsilanes: synthesis, properties, and applications. *Chem. Soc. Rev.* **2016,** 45 (19), 5358-5407.

24. Massey, J. A.; Temple, K.; Cao, L.; Rharbi, Y.; Raez, J.; Winnik, M. A.; Manners, I. Self-Assembly of Organometallic Block Copolymers: The Role of Crystallinity of the Core-Forming Polyferrocene Block

in the Micellar Morphologies Formed by Poly(ferrocenylsilane-b-dimethylsiloxane) in n-Alkane Solvents. *J. Am. Chem. Soc.* **2000,** 122 (47), 11577-11584.

25. Schmelz, J.; Schedl, A. E.; Steinlein, C.; Manners, I.; Schmalz, H. Length Control and Block-Type Architectures in Worm-like Micelles with Polyethylene Cores. *J. Am. Chem. Soc.* **2012,** 134 (34), 14217-14225.

26. Schmalz, H.; Schmelz, J.; Drechsler, M.; Yuan, J.; Walther, A.; Schweimer, K.; Mihut, A. M. Thermo-Reversible Formation of Wormlike Micelles with a Microphase-Separated Corona from a Semicrystalline Triblock Terpolymer. *Macromolecules* **2008,** 41 (9), 3235-3242.

27. Yin, L.; Lodge, T. P.; Hillmyer, M. A. A Stepwise "Micellization–Crystallization" Route to Oblate Ellipsoidal, Cylindrical, and Bilayer Micelles with Polyethylene Cores in Water. *Macromolecules* **2012,** 45 (23), 9460-9467.

28. Schöbel, J.; Karg, M.; Rosenbach, D.; Krauss, G.; Greiner, A.; Schmalz, H. Patchy Wormlike Micelles with Tailored Functionality by Crystallization-Driven Self-Assembly: A Versatile Platform for Mesostructured Hybrid Materials. *Macromolecules* **2016,** 49 (7), 2761-2771.

29. Mihut, A. M.; Drechsler, M.; Möller, M.; Ballauff, M. Sphere-to-Rod Transition of Micelles formed by the Semicrystalline Polybutadiene-block-Poly(ethylene oxide) Block Copolymer in a Selective Solvent. *Macromol. Rapid Commun.* **2010,** 31 (5), 449-453.

30. Du, Z.-X.; Xu, J.-T.; Fan, Z.-Q. Micellar Morphologies of Poly(ε-caprolactone)-b-poly(ethylene oxide) Block Copolymers in Water with a Crystalline Core. *Macromolecules* **2007,** 40 (21), 7633-7637.

31. He, W.-N.; Zhou, B.; Xu, J.-T.; Du, B.-Y.; Fan, Z.-Q. Two Growth Modes of Semicrystalline Cylindrical Poly(ε-caprolactone)-b-poly(ethylene oxide) Micelles. *Macromolecules* **2012,** 45 (24), 9768-9778.

32. Arno, M. C.; Inam, M.; Coe, Z.; Cambridge, G.; Macdougall, L. J.; Keogh, R.; Dove, A. P.; O'Reilly, R. K. Precision Epitaxy for Aqueous 1D and 2D Poly(ε-caprolactone) Assemblies. *J. Am. Chem. Soc.* **2017,** 139 (46), 16980-16985.

33. Petzetakis, N.; Walker, D.; Dove, A. P.; O'Reilly, R. K. Crystallization-driven sphere-to-rod transition of poly(lactide)-b-poly(acrylic acid) diblock copolymers: mechanism and kinetics. *Soft Matter* **2012,** 8 (28), 7408-7414.

34. Petzetakis, N.; Dove, A. P.; O'Reilly, R. K. Cylindrical micelles from the living crystallization-driven self-assembly of poly(lactide)-containing block copolymers. *Chem. Sci.* **2011,** 2 (5), 955-960.

35. Sun, L.; Petzetakis, N.; Pitto-Barry, A.; Schiller, T. L.; Kirby, N.; Keddie, D. J.; Boyd, B. J.; O'Reilly, R. K.; Dove, A. P. Tuning the Size of Cylindrical Micelles from Poly(l-lactide)-b-poly(acrylic acid) Diblock Copolymers Based on Crystallization-Driven Self-Assembly. *Macromolecules* **2013,** 46 (22), 9074-9082.

36. Fu, J.; Luan, B.; Yu, X.; Cong, Y.; Li, J.; Pan, C.; Han, Y.; Yang, Y.; Li, B. Self-Assembly of Crystalline−Coil Diblock Copolymer in Solvents with Varying Selectivity: From Spinodal-like Aggregates to Spheres, Cylinders, and Lamellae. *Macromolecules* **2004,** 37 (3), 976-986.

37. Yu, W.; Inam, M.; Jones, J. R.; Dove, A. P.; O'Reilly, R. K. Understanding the CDSA of poly(lactide) containing triblock copolymers. *Polym. Chem.* **2017,** 8 (36), 5504-5512.

38. Inam, M.; Cambridge, G.; Pitto-Barry, A.; Laker, Z. P. L.; Wilson, N. R.; Mathers, R. T.; Dove, A. P.; O'Reilly, R. K. 1D vs. 2D shape selectivity in the crystallization-driven self-assembly of polylactide block copolymers. *Chem. Sci.* **2017,** 8 (6), 4223-4230.

39. Gwyther, J.; Gilroy, J. B.; Rupar, P. A.; Lunn, D. J.; Kynaston, E.; Patra, S. K.; Whittell, G. R.; Winnik, M. A.; Manners, I. Dimensional Control of Block Copolymer Nanofibers with a π-Conjugated Core: Crystallization-Driven Solution Self-Assembly of Amphiphilic Poly(3-hexylthiophene)-b-poly(2-vinylpyridine). *Chem. Eur. J.* **2013,** 19 (28), 9186-9197.

40. Gilroy, J. B.; Lunn, D. J.; Patra, S. K.; Whittell, G. R.; Winnik, M. A.; Manners, I. Fiber-like Micelles via the Crystallization-Driven Solution Self-Assembly of Poly(3-hexylthiophene)-block-Poly(methyl methacrylate) Copolymers. *Macromolecules* **2012,** 45 (14), 5806-5815.

41. Patra, S. K.; Ahmed, R.; Whittell, G. R.; Lunn, D. J.; Dunphy, E. L.; Winnik, M. A.; Manners, I. Cylindrical Micelles of Controlled Length with a π-Conjugated Polythiophene Core via Crystallization-Driven Self-Assembly. *J. Am. Chem. Soc.* **2011,** 133 (23), 8842-8845.

42. Qian, J.; Li, X.; Lunn, D. J.; Gwyther, J.; Hudson, Z. M.; Kynaston, E.; Rupar, P. A.; Winnik, M. A.; Manners, I. Uniform, High Aspect Ratio Fiber-like Micelles and Block Co-micelles with a Crystalline π-Conjugated Polythiophene Core by Self-Seeding. *J. Am. Chem. Soc.* **2014,** 136 (11), 4121-4124.

43. Kamps, A. C.; Fryd, M.; Park, S.-J. Hierarchical Self-Assembly of Amphiphilic Semiconducting Polymers into Isolated, Bundled, and Branched Nanofibers. *ACS Nano* **2012,** 6 (3), 2844-2852.

44. Park, S.-J.; Kang, S.-G.; Fryd, M.; Saven, J. G.; Park, S.-J. Highly Tunable Photoluminescent Properties of Amphiphilic Conjugated Block Copolymers. *J. Am. Chem. Soc.* **2010,** 132 (29), 9931-9933.

45. Lee, E.; Hammer, B.; Kim, J.-K.; Page, Z.; Emrick, T.; Hayward, R. C. Hierarchical Helical Assembly of Conjugated Poly(3-hexylthiophene)-block-poly(3-triethylene glycol thiophene) Diblock Copolymers. *J. Am. Chem. Soc.* **2011,** 133 (27), 10390-10393.

46. Kynaston, E. L.; Gould, O. E. C.; Gwyther, J.; Whittell, G. R.; Winnik, M. A.; Manners, I. Fiber-Like Micelles from the Crystallization-Driven Self-Assembly of Poly(3-heptylselenophene)-block-Polystyrene. *Macromol. Chem. Phys.* **2015,** 216 (6), 685-695.

47. Wang, H.; Wang, H. H.; Urban, V. S.; Littrell, K. C.; Thiyagarajan, P.; Yu, L. Syntheses of Amphiphilic Diblock Copolymers Containing a Conjugated Block and Their Self-Assembling Properties. *J. Am. Chem. Soc.* **2000,** 122 (29), 6855-6861.

48. Tao, D.; Feng, C.; Cui, Y.; Yang, X.; Manners, I.; Winnik, M. A.; Huang, X. Monodisperse Fiber-like Micelles of Controlled Length and Composition with an Oligo(p-phenylenevinylene) Core via "Living" Crystallization-Driven Self-Assembly. *J. Am. Chem. Soc.* **2017,** 139 (21), 7136-7139.

49. Shin, S.; Menk, F.; Kim, Y.; Lim, J.; Char, K.; Zentel, R.; Choi, T.-L. Living Light-Induced Crystallization-Driven Self-Assembly for Rapid Preparation of Semiconducting Nanofibers. *J. Am. Chem. Soc.* **2018**, 140 (19), 6088-6094.

50. Tung, Y.-C.; Wu, W.-C.; Chen, W.-C. Morphological Transformation and Photophysical Properties of Rod-Coil Poly[2,7-(9,9-dihexylfluorene)]-block-poly(acrylic acid) in Solution. *Macromol. Rapid Commun.* **2006,** 27 (21), 1838-1844.

51. Lin, C.-H.; Tung, Y.-C.; Ruokolainen, J.; Mezzenga, R.; Chen, W.-C. Poly[2,7-(9,9-dihexylfluorene)]-block-poly(2-vinylpyridine) Rod−Coil and Coil−Rod−Coil Block Copolymers: Synthesis, Morphology and Photophysical Properties in Methanol/THF Mixed Solvents. *Macromolecules* **2008,** 41 (22), 8759-8769.

52. Tian, Y.; Chen, C.-Y.; Yip, H.-L.; Wu, W.-C.; Chen, W.-C.; Jen, A. K. Y. Synthesis, Nanostructure, Functionality, and Application of Polyfluorene-block-poly(N-isopropylacrylamide)s. *Macromolecules* **2010,** 43 (1), 282-291.

53. Gilroy, J. B.; Gädt, T.; Whittell, G. R.; Chabanne, L.; Mitchels, J. M.; Richardson, R. M.; Winnik, M. A.; Manners, I. Monodisperse cylindrical micelles by crystallization-driven living self-assembly. *Nat. Chem.* **2010,** 2 (7), 566-570.

54. Wang, X.; Guerin, G.; Wang, H.; Wang, Y.; Manners, I.; Winnik, M. A. Cylindrical Block Copolymer Micelles and Co-Micelles of Controlled Length and Architecture. *Science* **2007,** 317 (5838), 644-647.

55. Gadt, T.; Ieong, N. S.; Cambridge, G.; Winnik, M. A.; Manners, I. Complex and hierarchical micelle architectures from diblock copolymers using living, crystallization-driven polymerizations. *Nat. Mater.* **2009,** 8 (2), 144-150.

56. Rupar, P. A.; Chabanne, L.; Winnik, M. A.; Manners, I. Non-Centrosymmetric Cylindrical Micelles by Unidirectional Growth. *Science* **2012,** 337 (6094), 559-562.

57. Qian, J.; Lu, Y.; Chia, A.; Zhang, M.; Rupar, P. A.; Gunari, N.; Walker, G. C.; Cambridge, G.; He, F.; Guerin, G.; Manners, I.; Winnik, M. A. Self-Seeding in One Dimension: A Route to Uniform Fiber-like Nanostructures from Block Copolymers with a Crystallizable Core-Forming Block. *ACS Nano* **2013,** 7 (5), 3754-3766.

58. Qian, J.; Guerin, G.; Lu, Y.; Cambridge, G.; Manners, I.; Winnik, M. A. Self-Seeding in One Dimension: An Approach To Control the Length of Fiberlike Polyisoprene–Polyferrocenylsilane Block Copolymer Micelles. *Angew. Chem., Int. Ed.* **2011,** 50 (7), 1622-1625.

59. Gilroy, J. B.; Rupar, P. A.; Whittell, G. R.; Chabanne, L.; Terrill, N. J.; Winnik, M. A.; Manners, I.; Richardson, R. M. Probing the Structure of the Crystalline Core of Field-Aligned, Monodisperse, Cylindrical Polyisoprene-block-Polyferrocenylsilane Micelles in Solution Using Synchrotron Small- and Wide-Angle X-ray Scattering. *J. Am. Chem. Soc.* **2011,** 133 (42), 17056-17062.

60. Hayward, D. W.; Gilroy, J. B.; Rupar, P. A.; Chabanne, L.; Pizzey, C.; Winnik, M. A.; Whittell, G. R.; Manners, I.; Richardson, R. M. Liquid Crystalline Phase Behavior of Well-Defined Cylindrical Block Copolymer Micelles Using Synchrotron Small-Angle X-ray Scattering. *Macromolecules* **2015,** 48 (5), 1579-1591.

61. Wang, H.; Lin, W.; Fritz, K. P.; Scholes, G. D.; Winnik, M. A.; Manners, I. Cylindrical Block Co-Micelles with Spatially Selective Functionalization by Nanoparticles. *J. Am. Chem. Soc.* **2007,** 129 (43), 12924-12925.

62. Qiu, H.; Hudson, Z. M.; Winnik, M. A.; Manners, I. Multidimensional hierarchical self-assembly of amphiphilic cylindrical block comicelles. *Science* **2015,** 347 (6228), 1329-1332.

63. Li, X.; Gao, Y.; Boott, C. E.; Winnik, M. A.; Manners, I. Non-covalent synthesis of supermicelles with complex architectures using spatially confined hydrogen-bonding interactions. *Nat. Commun.* **2015,** 6, 8127.

64. Li, X.; Gao, Y.; Harniman, R.; Winnik, M.; Manners, I. Hierarchical Assembly of Cylindrical Block Comicelles Mediated by Spatially Confined Hydrogen-Bonding Interactions. *J. Am. Chem. Soc.* **2016,** 138 (39), 12902-12912.

65. Hudson, Z. M.; Lunn, D. J.; Winnik, M. A.; Manners, I. Colour-tunable fluorescent multiblock micelles. *Nat. Commun.* **2014,** 5, 3372.

66. Schmelz, J.; Karg, M.; Hellweg, T.; Schmalz, H. General Pathway toward Crystalline-Core Micelles with Tunable Morphology and Corona Segregation. *ACS Nano* **2011,** 5 (12), 9523-9534.

67. He, X.; Hsiao, M.-S.; Boott, Charlotte E.; Harniman, Robert L.; Nazemi, A.; Li, X.; Winnik, Mitchell A.; Manners, I. Two-dimensional assemblies from crystallizable homopolymers with charged termini. *Nat. Mater.* **2017,** 16, 481.

68. He, X.; He, Y.; Hsiao, M.-S.; Harniman, R. L.; Pearce, S.; Winnik, M. A.; Manners, I. Complex and Hierarchical 2D Assemblies via Crystallization-Driven Self-Assembly of Poly(l-lactide) Homopolymers with Charged Termini. *J. Am. Chem. Soc.* **2017,** 139 (27), 9221-9228.

69. Zhang, W.; Jin, W.; Fukushima, T.; Saeki, A.; Seki, S.; Aida, T. Supramolecular Linear Heterojunction Composed of Graphite-Like Semiconducting Nanotubular Segments. *Science* **2011,** 334 (6054), 340-343.

70. Ogi, S.; Sugiyasu, K.; Manna, S.; Samitsu, S.; Takeuchi, M. Living supramolecular polymerization realized through a biomimetic approach. *Nat. Chem.* **2014,** 6 (3), 188-195.

71. Ogi, S.; Stepanenko, V.; Sugiyasu, K.; Takeuchi, M.; Würthner, F. Mechanism of Self-Assembly Process and Seeded Supramolecular Polymerization of Perylene Bisimide Organogelator. *J. Am. Chem. Soc.* **2015,** 137 (9), 3300-3307.

72. Pal, A.; Malakoutikhah, M.; Leonetti, G.; Tezcan, M.; Colomb-Delsuc, M.; Nguyen, V. D.; van der Gucht, J.; Otto, S. Controlling the Structure and Length of Self-Synthesizing Supramolecular Polymers through Nucleated Growth and Disassembly. *Angew. Chem., Int. Ed.* **2015,** 54 (27), 7852-7856.

73. Robinson, M. E.; Lunn, D. J.; Nazemi, A.; Whittell, G. R.; De Cola, L.; Manners, I. Length control of supramolecular polymeric nanofibers based on stacked planar platinum(ii) complexes by seeded-growth. *Chem. Commun.* **2015,** 51 (88), 15921-15924.

74. Aliprandi, A.; Mauro, M.; De Cola, L. Controlling and imaging biomimetic self-assembly. *Nat. Chem.* **2016,** 8 (1), 10-15.

75. Ma, X.; Zhang, Y.; Zhang, Y.; Liu, Y.; Che, Y.; Zhao, J. Fabrication of Chiral-Selective Nanotubular Heterojunctions through Living Supramolecular Polymerization. *Angew. Chem., Int. Ed.* **2016,** 55 (33), 9539-9543.

76. Robinson, M. E.; Nazemi, A.; Lunn, D. J.; Hayward, D. W.; Boott, C. E.; Hsiao, M.-S.; Harniman, R. L.; Davis, S. A.; Whittell, G. R.; Richardson, R. M.; De Cola, L.; Manners, I. Dimensional Control and

Morphological Transformations of Supramolecular Polymeric Nanofibers Based on Cofacially-Stacked Planar Amphiphilic Platinum(II) Complexes. *ACS Nano* **2017,** 11 (9), 9162-9175.

77. Yu, B.; Jiang, X.; Yin, J. Size-Tunable Nanosheets by the Crystallization-Driven 2D Self-Assembly of Hyperbranched Poly(ether amine) (hPEA). *Macromolecules* **2014,** 47 (14), 4761-4768.

78. Qiu, H.; Gao, Y.; Boott, C. E.; Gould, O. E. C.; Harniman, R. L.; Miles, M. J.; Webb, S. E. D.; Winnik, M. A.; Manners, I. Uniform patchy and hollow rectangular platelet micelles from crystallizable polymer blends. *Science* **2016,** 352 (6286), 697-701.

79. Han, L.; Wang, M.; Jia, X.; Chen, W.; Qian, H.; He, F. Uniform two-dimensional square assemblies from conjugated block copolymers driven by π–π interactions with controllable sizes. *Nat. Commun.* **2018,** 9 (1), 865.

80. Li, Z.; Ono, R. J.; Wu, Z.-Q.; Bielawski, C. W. Synthesis and self-assembly of poly(3-hexylthiophene)-block-poly(acrylic acid). *Chem. Commun.* **2011,** 47 (1), 197-199.

81. Tu, G.; Li, H.; Forster, M.; Heiderhoff, R.; Balk, L. J.; Sigel, R.; Scherf, U. Amphiphilic Conjugated Block Copolymers: Synthesis and Solvent-Selective Photoluminescence Quenching. *Small* **2007,** 3 (6), 1001-1006.

82. Lee, I.-H.; Amaladass, P.; Yoon, K.-Y.; Shin, S.; Kim, Y.-J.; Kim, I.; Lee, E.; Choi, T.-L. Nanostar and Nanonetwork Crystals Fabricated by in Situ Nanoparticlization of Fully Conjugated Polythiophene Diblock Copolymers. *J. Am. Chem. Soc.* **2013,** 135 (47), 17695-17698.

83. Jin, S.-M.; Kim, I.; Lim, J. A.; Ahn, H.; Lee, E. Interfacial Crystallization-Driven Assembly of Conjugated Polymers/Quantum Dots into Coaxial Hybrid Nanowires: Elucidation of Conjugated Polymer Arrangements by Electron Tomography. *Adv. Funct. Mater.* **2016,** 26 (19), 3226-3235.

84. Cativo, M. H. M.; Kim, D. K.; Riggleman, R. A.; Yager, K. G.; Nonnenmann, S. S.; Chao, H.; Bonnell, D. A.; Black, C. T.; Kagan, C. R.; Park, S.-J. Air–Liquid Interfacial Self-Assembly of Conjugated Block Copolymers into Ordered Nanowire Arrays. *ACS Nano* **2014,** 8 (12), 12755-12762.

85. Li, X.; Wolanin, P. J.; MacFarlane, L. R.; Harniman, R. L.; Qian, J.; Gould, O. E. C.; Dane, T. G.; Rudin, J.; Cryan, M. J.; Schmaltz, T.; Frauenrath, H.; Winnik, M. A.; Faul, C. F. J.; Manners, I. Uniform electroactive fibre-like micelle nanowires for organic electronics. *Nat. Commun.* **2017,** 8, 15909.

86. Kim, F. S.; Ren, G.; Jenekhe, S. A. One-Dimensional Nanostructures of π-Conjugated Molecular Systems: Assembly, Properties, and Applications from Photovoltaics, Sensors, and Nanophotonics to Nanoelectronics. *Chem. Mater.* **2011,** 23 (3), 682-732.

87. Lim, J. A.; Liu, F.; Ferdous, S.; Muthukumar, M.; Briseno, A. L. Polymer semiconductor crystals. *Mater. Today* **2010,** 13 (5), 14-24.

88. Kim, D. H.; Han, J. T.; Park, Y. D.; Jang, Y.; Cho, J. H.; Hwang, M.; Cho, K. Single-Crystal Polythiophene Microwires Grown by Self-Assembly. *Adv. Mater.* **2006,** 18 (6), 719-723.

89. The use of elevated temperatures to achieve more efficient living CDSA in 1D and 2D has been reported for several other core-forming blocks: see for example, references 34 and 78. While this manuscript was in preparation an example of the use of higher temperatures (30°C versus 23°C) to minimise self-nucleation was reported for 1D seeded growth of OPV BCPs see ref 48.

90. Jeffries-El, M.; Sauvé, G.; McCullough, R. D. Facile Synthesis of End-Functionalized Regioregular Poly(3-alkylthiophene)s via Modified Grignard Metathesis Reaction. *Macromolecules* **2005,** 38 (25), 10346-10352.

91. Miyakoshi, R.; Yokoyama, A.; Yokozawa, T. Catalyst-Transfer Polycondensation. Mechanism of Ni-Catalyzed Chain-Growth Polymerization Leading to Well-Defined Poly(3-hexylthiophene). *J. Am. Chem. Soc.* **2005,** 127 (49), 17542-17547.

92. Yokoyama, A.; Miyakoshi, R.; Yokozawa, T. Chain-Growth Polymerization for Poly(3-hexylthiophene) with a Defined Molecular Weight and a Low Polydispersity. *Macromolecules* **2004,** 37 (4), 1169-1171.

93. Zhang, M.; Rupar, P. A.; Feng, C.; Lin, K.; Lunn, D. J.; Oliver, A.; Nunns, A.; Whittell, G. R.; Manners, I.; Winnik, M. A. Modular Synthesis of Polyferrocenylsilane Block Copolymers by Cu-Catalyzed Alkyne/Azide “Click” Reactions. *Macromolecules* **2013,** 46 (4), 1296-1304.

94. Mao, H.; Xu, B.; Holdcroft, S. Synthesis and structure-property relationships of regioirregular poly(3-hexylthiophenes). *Macromolecules* **1993,** 26 (5), 1163-1169.

95. Chen, T.-A.; Wu, X.; Rieke, R. D. Regiocontrolled Synthesis of Poly(3-alkylthiophenes) Mediated by Rieke Zinc: Their Characterization and Solid-State Properties. *J. Am. Chem. Soc.* **1995,** 117 (1), 233-244.

96. Rughooputh, S. D. D. V.; Hotta, S.; Heeger, A. J.; Wudl, F. Chromism of soluble polythienylenes. *J. Polym. Sci., Part B: Polym. Phys.* **1987,** 25 (5), 1071-1078.

97. McCullough, R. D.; Lowe, R. D.; Jayaraman, M.; Anderson, D. L. Design, synthesis, and control of conducting polymer architectures: structurally homogeneous poly(3-alkylthiophenes). *J. Org. Chem.* **1993,** 58 (4), 904-912.

98. Chen, S. A.; Ni, J. M. Structure/properties of conjugated conductive polymers. 1. Neutral poly(3-alkythiophene)s. *Macromolecules* **1992,** 25 (23), 6081-6089.

99. Samitsu, S.; Shimomura, T.; Heike, S.; Hashizume, T.; Ito, K. Effective Production of Poly(3-alkylthiophene) Nanofibers by means of Whisker Method using Anisole Solvent: Structural, Optical, and Electrical Properties. *Macromolecules* **2008,** 41 (21), 8000-8010.

100. Liu, J.; Arif, M.; Zou, J.; Khondaker, S. I.; Zhai, L. Controlling Poly(3-hexylthiophene) Crystal Dimension: Nanowhiskers and Nanoribbons. *Macromolecules* **2009,** 42 (24), 9390-9393.

101. Zen, A.; Saphiannikova, M.; Neher, D.; Grenzer, J.; Grigorian, S.; Pietsch, U.; Asawapirom, U.; Janietz, S.; Scherf, U.; Lieberwirth, I.; Wegner, G. Effect of Molecular Weight on the Structure and Crystallinity of Poly(3-hexylthiophene). *Macromolecules* **2006,** 39 (6), 2162-2171.

102. Ihn, K. J.; Moulton, J.; Smith, P. Whiskers of poly(3-alkylthiophene)s. *J. Polym. Sci., Part B: Polym. Phys.* **1993,** 31 (6), 735-742.

103. Wu, P.-T.; Ren, G.; Li, C.; Mezzenga, R.; Jenekhe, S. A. Crystalline Diblock Conjugated Copolymers: Synthesis, Self-Assembly, and Microphase Separation of Poly(3-butylthiophene)-b-poly(3-octylthiophene). *Macromolecules* **2009,** 42 (7), 2317-2320.

104. Surin, M.; Coulembier, O.; Tran, K.; Winter, J. D.; Leclère, P.; Gerbaux, P.; Lazzaroni, R.; Dubois, P. Regioregular poly(3-hexylthiophene)-poly(ε-caprolactone) block copolymers: Controlled synthesis, microscopic morphology, and charge transport properties. *Org. Electron.* **2010,** 11 (5), 767-774.

105. Xu, B.; Holdcroft, S. Molecular control of luminescence from poly(3-hexylthiophenes). *Macromolecules* **1993,** 26 (17), 4457-4460.

106. Finnegan, J. R.; Lunn, D. J.; Gould, O. E. C.; Hudson, Z. M.; Whittell, G. R.; Winnik, M. A.; Manners, I. Gradient Crystallization-Driven Self-Assembly: Cylindrical Micelles with "Patchy" Segmented Coronas via the Coassembly of Linear and Brush Block Copolymers. *J. Am. Chem. Soc.* **2014,** 136 (39), 13835-13844.

107. Kynaston, E. L.; Nazemi, A.; MacFarlane, L. R.; Whittell, G. R.; Faul, C. F. J.; Manners, I. Uniform Polyselenophene Block Copolymer Fiberlike Micelles and Block Co-micelles via Living Crystallization-Driven Self-Assembly. *Macromolecules* **2018,** 51 (3), 1002-1010.

For Table of Contents Use Only